

1 Article

2

Mesoscopic Modeling of Encapsulation of Capsaicin

3

by Lecithin/Chitosan Liposomal Nanoparticles

4 **Ketzasmin A. Terrón-Mejía ^{1,2}, Evelin Martínez-Benavidez ¹, Inocencio Higuera-Ciapara ¹, Claudia**
5 **Virués ³, Javier Hernández ⁴, Zaira Domínguez ⁴, W. Argüelles-Monal ⁵, Francisco M. Goycoolea ⁶,**
6 **Roberto López-Rendón ^{7*}, and Armando Gama Goicochea ^{8*}**7 ¹ Centro de Investigación y Asistencia en Tecnología y Diseño del Estado de Jalisco, A.C., Av. Normalistas
8 800, Colinas de la Normal, Guadalajara, Jalisco, 44270, México; (K.A.T.-M. : ket.a.t.m@gmail.com), (E.M.-B.
9 : emartinez@ciatej.mx), (I.H.-C. : inohiguera@ciatej.mx)10 ² Instituto Tecnológico Superior de Zongolica, Km. 4 Carretera a la Compañía, Zongolica, Veracruz, 95005,
11 México; (K.A.T.-M. : ket.a.t.m@gmail.com)12 ³ Centro de Investigación y Asistencia en Tecnología y Diseño del Estado de Jalisco, A.C., Clúster Científico
13 y Tecnológico Biomimic®, Carretera antigua a Coatepec No. 351, Colonia El Haya, Xalapa, Veracruz 91070,
14 México; (cvirues@ciatej.mx)15 ⁴ Unidad de Servicios de Apoyo en Resolución Analítica, Universidad Veracruzana, Apartado Postal 575,
16 Xalapa, Veracruz, 91190, México; (J.H. : javmartinez@uv.mx), (Z.D. : zdominguez@uv.mx)17 ⁵ Centro de Investigación en Alimentación y Desarrollo A. C., Grupo de Investigación en Biopolímeros,
18 Carr. a La Victoria km. 0.6, Hermosillo, Sonora, 83304, México; waldo@ciad.mx19 ⁶ School of Food Science and Nutrition. University of Leeds. Woodhouse Ln, Leeds LS2 9JT, United
20 Kingdom; F.M.Goycoolea@leeds.ac.uk21 ⁷ Laboratorio de Bioingeniería Molecular a Multiescala, Facultad de Ciencias, Universidad Autónoma del
22 Estado de México, Av. Instituto Literario 100, Toluca, Estado de México, 50000, México;
roberto.lopez.rendon@gmail.com23 ⁸ División de Ingeniería Química y Bioquímica, Tecnológico de Estudios Superiores de Ecatepec, Av.
24 Tecnológico s/n, Ecatepec, Estado de México, 55210, México; agama@alumni.stanford.edu25 * Correspondence: agama@alumni.stanford.edu; roberto.lopez.rendon@gmail.com; Tel.: +52-555-000-2300,
26 and +52-722-296-5554

27

28 **Abstract:** Transport of hydrophobic drugs in the human body exhibits complications due to the low
29 solubility of these compounds. With the purpose of enhancing the bioavailability and
30 biodistribution of such drugs, recent studies have reported the use of amphiphilic molecules, such
31 as phospholipids, for synthesis of nanoparticles or nanocapsules. Given that phospholipids can self-
32 assemble in liposomes or micellar structures, they are ideal candidates to function as vehicles of
33 hydrophobic molecules. In this work, we report mesoscopic simulations of nanoliposomes,
34 constituted by lecithin and coated with a shell of chitosan. The stability of such structure and the
35 efficiency of encapsulation of capsaicin, as well as the internal and superficial distribution of
36 capsaicin and chitosan inside the nanoliposome were analyzed. The characterization of the system
37 was carried out through density maps and the potentials of mean force for the lecithin–capsaicin,
38 lecithin–chitosan and capsaicin–chitosan interactions. The results of these simulations show that
39 chitosan is deposited on the surface of the nanoliposome, as has been reported in some experimental
40 works. It was also observed that a nanoliposome of approximately 18 nm in diameter is stable
41 during the simulation. The deposition behavior was found to be influenced by pattern of N-
42 acetylation of chitosan.
4344
45 **Keywords:** capsaicin; chitosan; lecithin; dissipative particle dynamics

46

47

48 1. Introduction

49 The advent of nanobiotechnology has seen increasing research and development in the use of
50 bioconjugates as new therapeutic alternatives [1]. One of the main goal of these technologies is to
51 focus on utilizing inherent structural, specific recognition or catalytic properties of biomolecules to
52 assemble composite nanoscale materials or devices with unique or novel properties [2]. For instance,
53 several carriers, comprised by biopolymers, macromolecules and liposomes have been used to
54 deliver drugs *in vivo* [3]. Liposomes are microscopic vesicles formed essentially by phospholipids
55 dispersed in water, which are amphiphilic molecules containing polar heads and hydrophobic
56 hydrocarbon tails with the ability to self-associate spontaneously and form bilayer vesicles [4].

57 The use of colloidal carriers made of hydrophilic polysaccharides, i.e. chitosan (CS), has arisen
58 as a promising alternative for improving the transport of therapeutic peptides, proteins,
59 oligonucleotides, and plasmids across biological surfaces [5]. CS is the common name of a linear,
60 random copolymer of β -(1-4)-linked D-glucosamine and N-acetyl-D-glucosamine whose molecular
61 structure comprises a linear backbone linked through glycosidic bonds. CS is a hydrophilic,
62 biocompatible, and biodegradable polymer of low toxicity. Recent reviews have highlighted the
63 potential use of CS-based drug deliverers [6, 7]. Also, the characteristics of CS-coated liposomes and
64 their interactions with leuprolide have been investigated by Gou et al. [8].

65 On the other hand, lecithin, which has two long hydrocarbon chains, is a major component of
66 lipid bilayers of cell membranes and a natural, biological amphiphile. Lecithin is a natural lipid
67 mixture of phospholipids and is frequently used for the preparation of various nanosystem delivery
68 vehicles, such as microemulsions, liposomes, micelles, and nanoparticles, and is considered to be a
69 safe and biocompatible excipient [9, 10, 11]. The potential of the various applications that have been
70 found in lecithin/CS nanoparticles has already been reported, for instance, its potential as a
71 mucoadhesive colloidal nanosystem for transmucosal delivery of melatonin was investigated [12] as
72 a topical delivery system for quercetin [13]. The encapsulation of quercetin into lecithin/CS
73 nanoparticles [14] and chitosan-coated nanocapsules [15], as well as the influence of loaded tamoxifen
74 on the structure of lecithin/CS nanoparticles has also been investigated [16]. Other nanostructured
75 materials that harness the interactions of lecithin phospholipid/CS have comprised electrospun
76 nanofibers [17] and nanoporous hydrogels [18].

77 Capsaicin (8-methyl-N-vanillyl-6-nonenamide), a lipophilic drug, is the pungent vanilloid
78 compound in spicy chili peppers. It is also approved as a drug for the treatment of chronic pains (e.g.
79 arthritis, migraine, diabetic neuropathy) [19, 20] and its potential use in the treatment of urological
80 disorders, control of satiety and obesity [21], has also been documented. Capsaicin is known to be an
81 agonist of the transient receptor potential vanilloid 1 (TRPV1), a nonselective cation channel which
82 is involved in the detection of body temperature and heat nociception [22]. Capsaicin has a
83 nociceptive-blocking action that is the basis of its pharmacological use as an analgesic in persistent
84 pathological pain states [23].

85 In light of the well-established pharmacological activities of capsaicin, identifying new potential
86 nanocarriers for intracellular, transdermal and/or for intranasal delivery of capsaicin, so as to regulate
87 the activity of its receptors in various tissues, appeals as a potential emerging therapeutic strategy.
88 However, the handling and administration of capsaicin is not always feasible due to its pungency,
89 cytotoxicity at high concentrations [24], and sparing solubility in water [25]. Several studies have been
90 conducted to incorporate capsaicin into nanoformulations in an attempt to make it more compatible
91 with aqueous physiological environments [26, 27]. For instance, capsaicin-loaded nanoemulsions
92 stabilized with natural biopolymer such as alginate and CS has been used as a functional ingredient
93 delivery system [28]. We have encapsulated capsaicin using oil-core CS-based nanocapsules and
94 examined the effect on modulating its pungency [27, 29], just to mention a few studies.

95 Notwithstanding the aforementioned, the use of nanostructured materials or functionalized
96 nanocarriers with biopolymers, has received a great deal of attention. Recent studies show that
97 biopolymers, such as CS or cellulose and modifications of these, are ideal candidates for developing
98 improved nanocapsules [30, 31], with increased efficiency in the delivery of different drugs, mainly

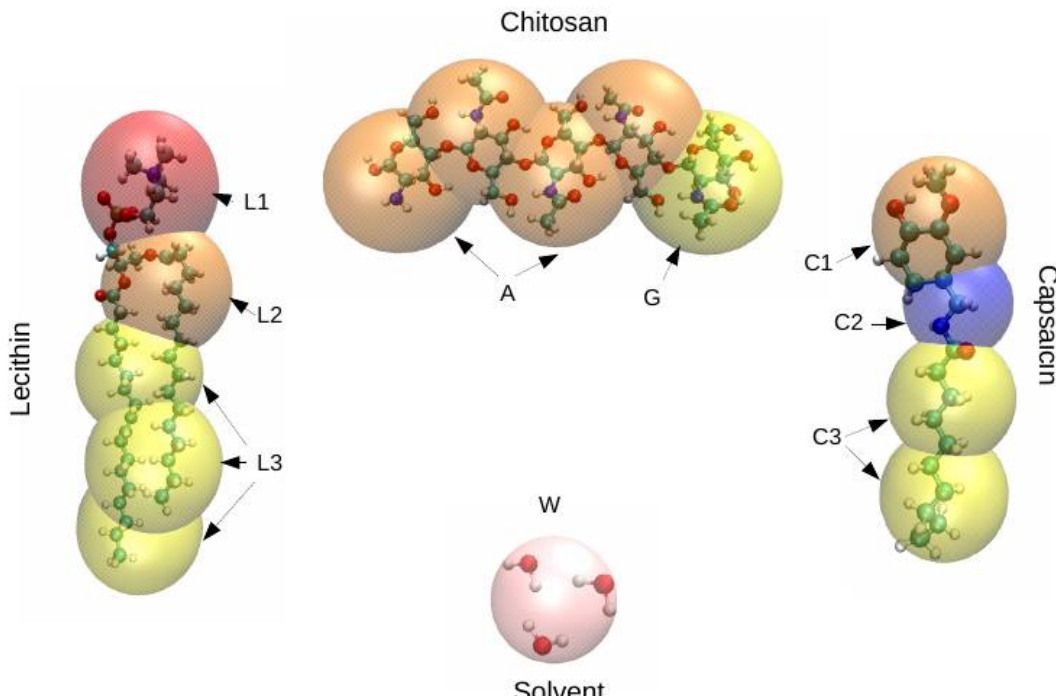
99 of the hydrophobic type [32]. These drugs have very low solubility, hence its biodistribution is very
100 limited if there is no suitable vehicle for administration. Thus, nanocapsules represent a very good
101 option to solve this problem. In addition, colloidal nanocapsules with an oily core and a CS shell have
102 been investigated as potential nanocarriers for transmucosal drug delivery [33]. These systems
103 assemble by spontaneous emulsification [34, 35] and are versatile because they can carry both
104 lipophilic and hydrophilic macromolecules [36, 37].

105 Experimental work [38, 39] has shown compatibility between lecithin/CS liposomal
106 nanoparticles as nanocarriers. Coated liposomes may subsequently be of significant interest to food
107 and pharmaceutical industries for the improved delivery of lipophilic and hydrophilic functional
108 components such as flavors, antioxidants, antimicrobials, and bioactives [40]. However, at the
109 molecular level it has been difficult to elucidate, the nature of the interactions between these
110 components to optimize the formation of nanocapsules. On the other hand, one can dispose of the
111 methods of computational modeling that are available to study such interactions [41]. These tools
112 have shown to be quite effective in the prediction of physicochemical and structural properties of
113 complex systems [42, 43]. Thus, the goal of the current work was to use mesoscopic simulations
114 through the approach of dissipative particle dynamics (DPD) to analyze and characterize
115 nanocapsules constituted by nanoliposomes of lecithin coated with a shell of CS and its function as
116 nanocarriers for the administration of capsaicin, which has proven applications in some therapies.

117 The remainder of this paper is organized as follows. The models and methods are detailed in
118 Section 2. The results and discussion are presented in Section 3. Finally, the conclusions are drawn in
119 Section 4. The general equations of the DPD approach, the simulation methodology, and full details
120 of our models presented in this work can be found in the supplementary information (SI) that
121 accompanies this paper.

122 2. Models and Methods

123 DPD is a mesoscopic technique previously shown to be successful in the prediction of
124 equilibrium and non-equilibrium properties of soft matter systems [44, 45], which makes it suitable
125 to study the coating of nanoliposomes by CS. The numerical simulations presented in this work were
126 carried out in the canonical assemble (constant density and temperature), with the global density set
127 equal to three, as is usually done. Molecules of lecithin, capsaicin and CS were derived from atomic
128 structure in a coarse-graining molecular model, as show in Figure 1. For practical purposes, particles
129 in the coarse-graining models are interpreted as groups of atoms instead of individual atoms. The
130 details of this parametrization are in the SI that accompanies this document. All simulations reported
131 here were performed with our software, SIMES [46], which is designed to run simulations completely
132 on graphic processing units (GPUs), under the DPD framework.



133

134 **Figure 1. (Color online). Schematic representation of the coarse-grained models adopted in this**
 135 **work.** Mesoscopic models for lecithin (left), CS (center up), water as solvent (center down) and
 136 capsaicin (right). The exact division of every functional group is presented in the SI. In overview, the
 137 molecular structure of lecithin is composed of three different beads that we have labelled as *L*1, *L*2,
 138 and *L*3, that correspond to head, neck and tail groups respectively. The same nomenclature is used
 139 for capsaicin, where the beads *C*1, *C*2, and *C*3 correspond to the head, neck, and tail groups
 140 respectively. The CS model consists of two types of beads, the first bead represents the glucosamine
 141 units, which are labelled *G*, while the second bead represents the *N*-acetyl-glucosamine units, which
 142 are labelled *A*. Finally, the solvent (water) is represented by bead *W*. These Figures were prepared
 143 with VMD package [47].

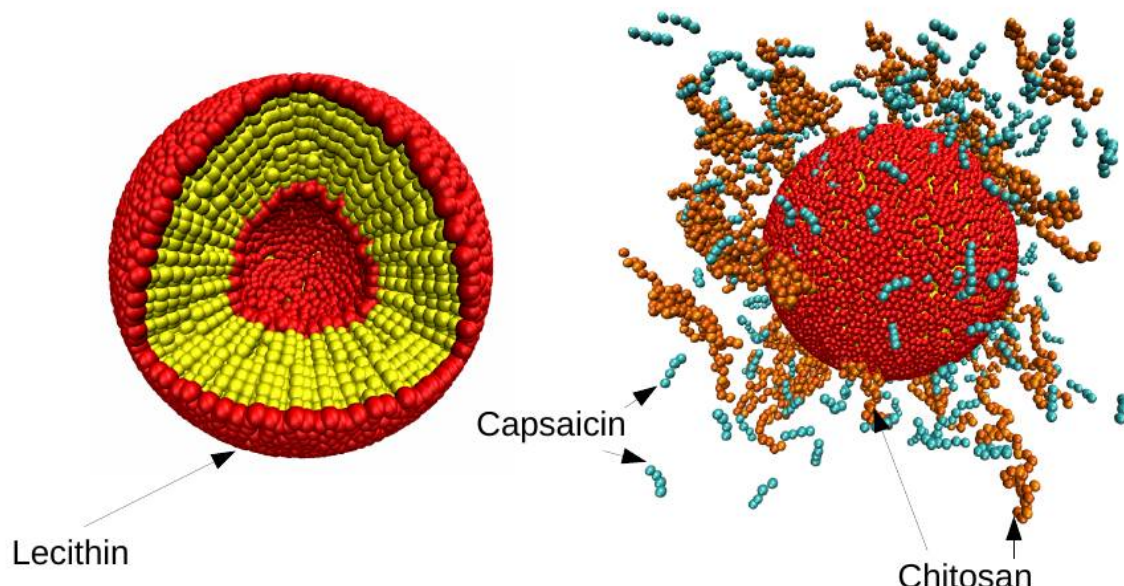
144 **3. Results and discussion**

145 The simulations are performed starting from an initial configuration of the liposome as shown
 146 in Figure 2 (left). This liposome is found in aqueous solution together with capsaicin molecules and
 147 polymeric chains of CS, which are dispersed in a random configuration, as shown in Figure 2 (right).
 148 The simulations carried out in this work are divided into two sets: the first one consists of keeping
 149 the concentration of capsaicin fixed and exploring the behavior of the nanocapsule as a function of
 150 CS concentration in solution. The second set involves CS and we explored the influence of the degree
 151 of deacetylation (DA) by changing the polymer sequence, as is described below. The degree of
 152 deacetylation represents the proportion of glucosamine units (deacetylated monomers) in a CS
 153 polymer molecule. The DA of CS is an important characterization parameter since it influences
 154 several physicochemical properties [48, 49]. For this second case, the distribution of *N*-acetyl-D-
 155 glucosamine (GlucNA) and D-glucosamine groups (GlcN), over the CS chain affects the properties
 156 of the polymer. It also allows the appearance of cooperative effects due to the association of
 157 hydrophobic units with the concomitant effect over the properties of nanocapsules. To achieve this
 158 purpose, we explored two different sequences (S1 and S2) in the CS polymer, the first (S1) was more
 159 random than the second (S2). Both sequences maintained a degree of *N*-acetylation of 30%. The CS
 160 monomer sequences considered in the simulations were prepared as follows:
 161

162 a)[-GlucNA - [GlcN]₃ - GlucNA - [GlcN]₃ - GlucNA - GlcN -]

163 b) $-[\text{GlucNA}_4 - [\text{GlcN}_9]_3 - [\text{GlucNA}]_3 - [\text{GlcN}]_8$

164 According to this nomenclature, the first sequence consists of five blocks. Each of these blocks
 165 was composed of a unit of GlucNA, followed by three units of GlcN. These two sections are repeated
 166 and the sequence ends with a GlucNA unit linked to GlcN. The second sequence is composed of three
 167 sections. The first section consists of three blocks, which are formed by four units of GlucNA bonded
 168 to nine units GlcN. The second section contains three units of GlucNA, while the third section
 169 contains eight units of GlcN.



170

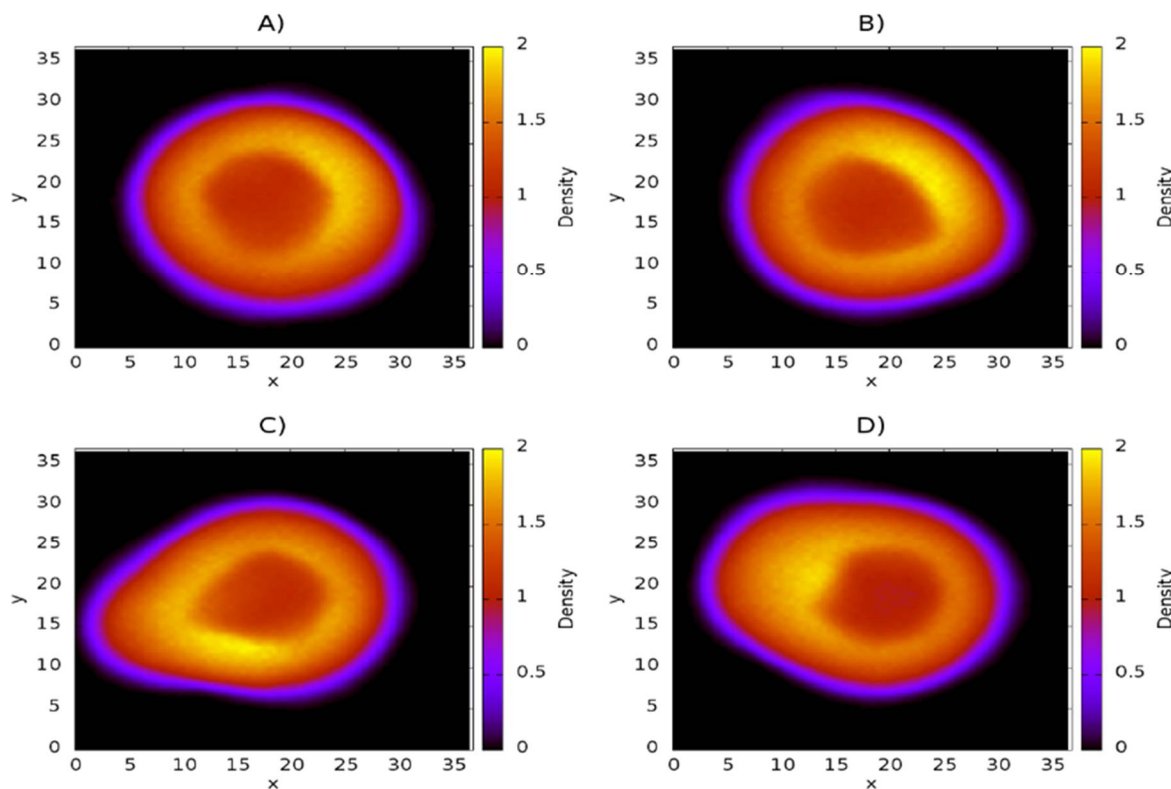
171 **Figure 2. (Color online). Initial configuration of nanoliposome.** A snapshot of the initial
 172 configuration of lecithin molecules into the structure of a liposome bilayer (left). The yellow spheres
 173 represent the hydrophobic part, while the red spheres represent the hydrophilic part of the lecithin.
 174 The capsaicin and CS molecules were placed in a random configuration around the lecithin (right).
 175 The orange chains represent the CS polymers, while the turquoise chains represent the capsaicin
 176 molecules. These Figures were prepared with the VMD package [47].

177 Influence of chitosan concentration on lecithin

178 Density maps corresponding to lecithin, CS and capsaicin were obtained from the simulations.
 179 These density maps, mainly of lecithin, are useful to determine if the structure of the liposome was
 180 affected by the presence of CS or capsaicin. First, the concentration of capsaicin in the system (250
 181 molecules of capsaicin) was fixed and then the concentration of CS was changed, starting with 50
 182 chains up to a total of 200 chains, in increments of 50 chains. These amounts of CS correspond to
 183 concentrations of 6, 12, 18 and 24 mM respectively. The density maps of lecithin as function of CS
 184 concentration are shown in Figure 3. They show the structure of the liposome, as well as the region
 185 formed by the lipid membrane which is presented as the region with the highest concentration (in
 186 yellow) in the four cases. From these maps it is possible to observe that the core zone shows a more
 187 reddish tone, which indicates that the lipid density is lower, as expected. Density maps also show
 188 that the nanoliposome is stable during 24 μ s of simulation, since the lecithin molecules do not spread
 189 all over the simulation box, nor do they collapse in the aqueous core to form a micelle.

190 In regard to the increase of CS in the system, Figure 3-A) shows that the structure of the
 191 nanoliposome is not affected by CS; even more, the nanoliposome remains quasi spherically
 192 symmetrical. Figure 3-B) shows the nanoliposome undergoes minimal alteration in its structure,
 193 losing some spherical symmetry. Figure 3-C) shows a pronounced protuberance in the

194 nanoliposome, located in the interval (5, 10) along the x coordinate. In this case the lipid membrane
 195 could break, thus influencing the structural stability of the nanoliposome. In Figure 3-D) a
 196 protuberance similar to that shown in Figure 3-C) occurs. Under these conditions, the liposome
 197 membrane is thicker.

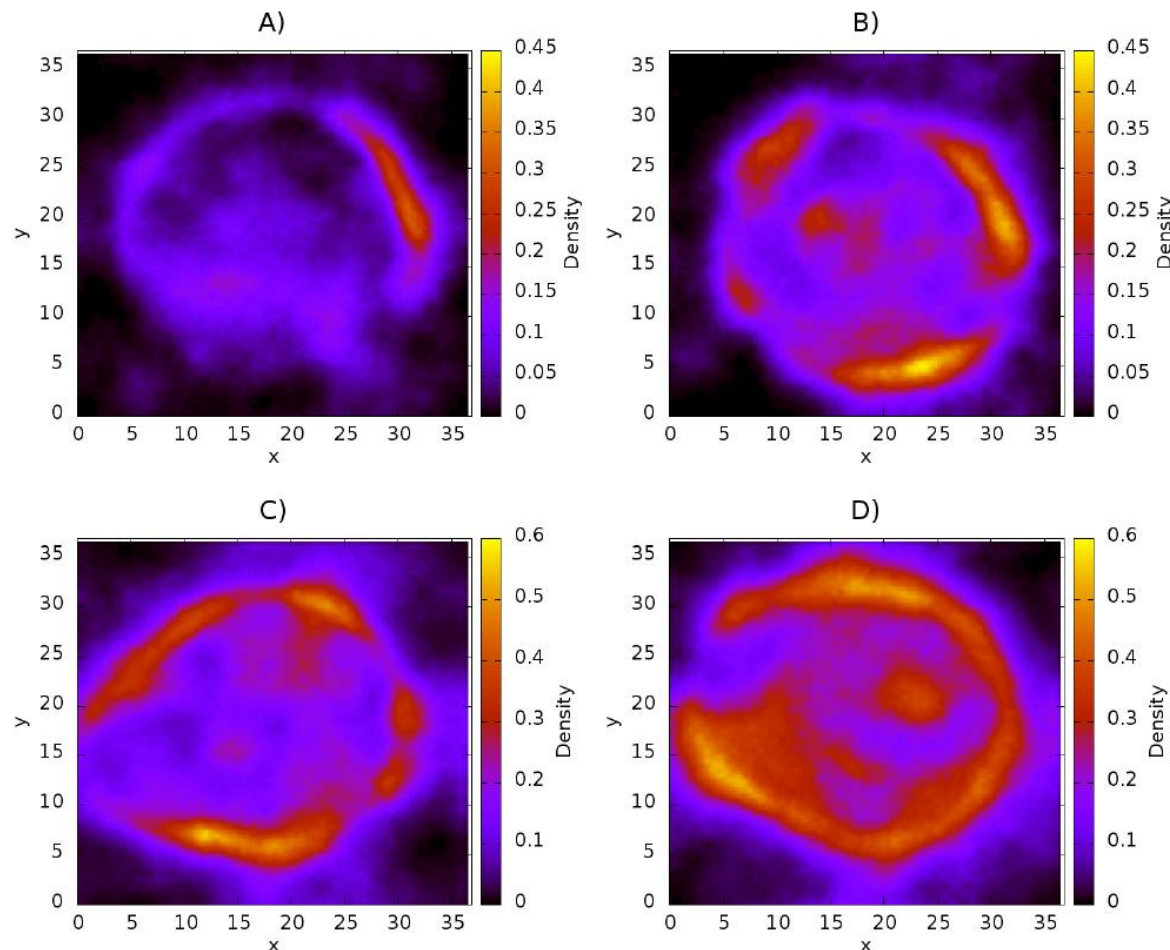


198

199 **Figure 3.** Density maps of lecithin on the xy plane at different concentration of CS. A) 50 chains of CS
 200 (6 mM). B) 100 chains of CS (12 mM). C) 150 chains of CS (18 mM). D) 200 chains of CS (24 mM). The
 201 scale of density bars starts at 0.0 (black regions) and reaches the maximum at 2.0 (yellow regions). All
 202 quantities are expressed in reduced DPD units.

203 Distribution of chitosan on liposome

204 The density maps corresponding to CS are shown in Figure 4. These maps show that CS is
 205 adsorbed over the surface of the nanoliposome, as has been reported in experimental work [50-52]. It
 206 is also possible to see how the surface becomes more homogeneous with increasing CS concentration.
 207 Figure 4-A) shows that the CS concentration is not sufficient to cover the surface of the nanoliposome,
 208 since the area comprising the radius of the nanoliposome exhibits regions of very low density, which
 209 indicates a deficiency of polymeric chains in the zone. Figure 4-B) shows that increasing the
 210 concentration in 50 CS chains, equivalent to a concentration of 12 mM, the nanoliposome becomes
 211 uniformly coated by the polymer. The appearance of yellow regions are indicative of an association
 212 of CS polymers. Figure 4-C) shows the distribution of CS at a concentration of 18 mM on the
 213 liposome. The regions of greater density are more pronounced than in the previous case. A greater
 214 adsorption of CS is observed too. In this case the polymer acts as a protective layer. The last case
 215 represents the adsorption of polymers of CS at a concentration of 24 mM. (Figure 4-D). Under this
 216 condition the surface of the liposome becomes almost completely coated. It is also possible to observe
 217 how an increasing concentration of CS, raises the quantity of supernatant polymer in the aqueous
 218 medium, thus indicating that a competitive association between CS-liposome and CS-CS is present.
 219 The blue regions refer to low density of CS, while the red regions refer to regions of high density of
 220 CS.

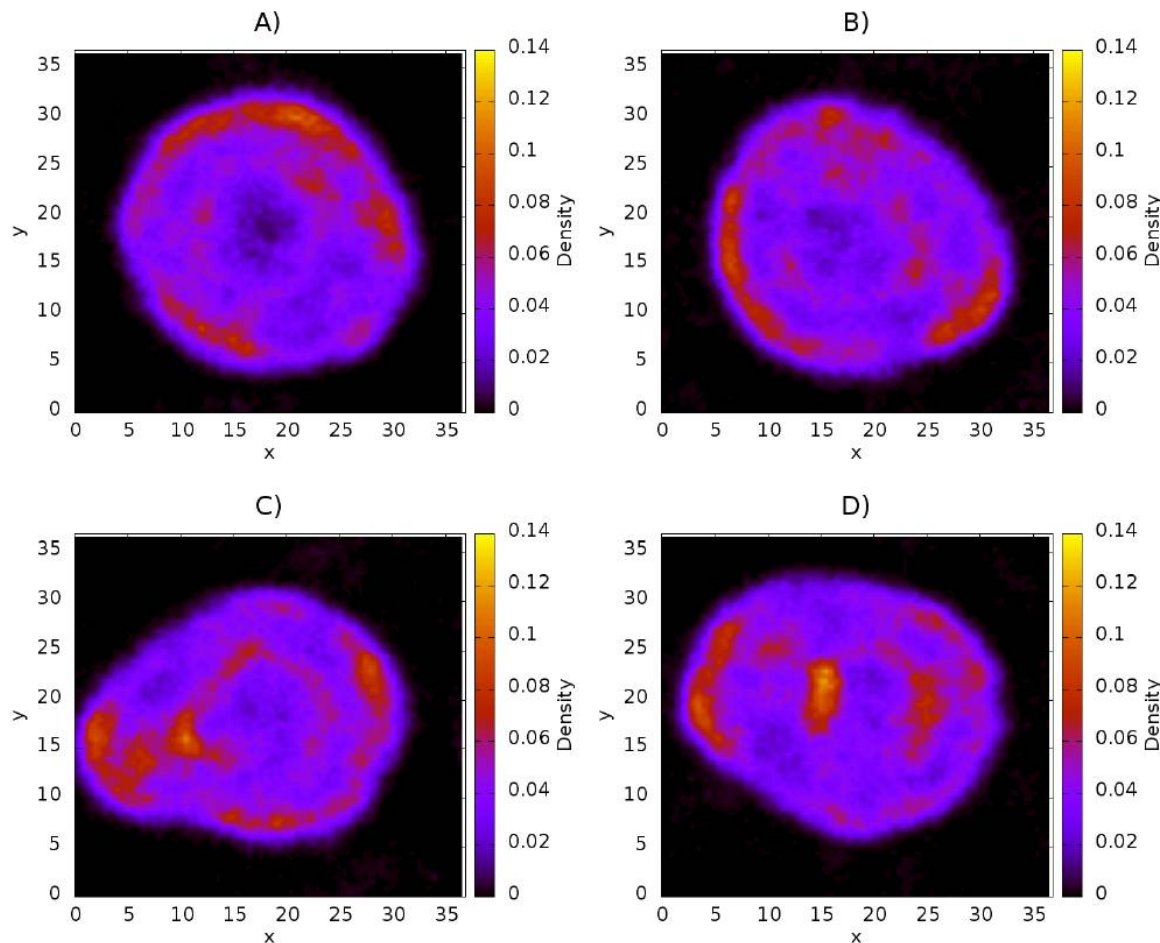


221

222 **Figure 4.** Distribution of CS on liposome on the xy plane. A) 50 chains of CS. B) 100 chains of CS, C)
223 150 chains of CS. D) 200 chains of CS. All quantities are reported in reduced DPD units.

224 **Influence of chitosan concentration on capsaicin**

225 Density maps corresponding to the capsaicin molecules are shown in Figure 5. These maps
226 clearly show that capsaicin is absorbed and encapsulated in the nanoliposome. This phenomenon is
227 not affected by the presence of the CS polymer, which indicates that interactions between capsaicin
228 and CS are very weak in comparison to the interactions between lecithin and capsaicin. In Figures 5–
229 A), 5–B), 5–C) and 5–D) it is possible observe how the capsaicin molecules are deposited close to
230 interface between the nanoliposome and the aqueous medium and even in the interface with the
231 aqueous core which suggests that capsaicin will be transported by the oil phase in the nanoliposome,
232 thus leaving free the aqueous core with capacity to transport other hydrophilic molecules with
233 therapeutic potential. If the capsaicin reached the core, a yellow or high density region would be
234 observed in the center, which does not occur.

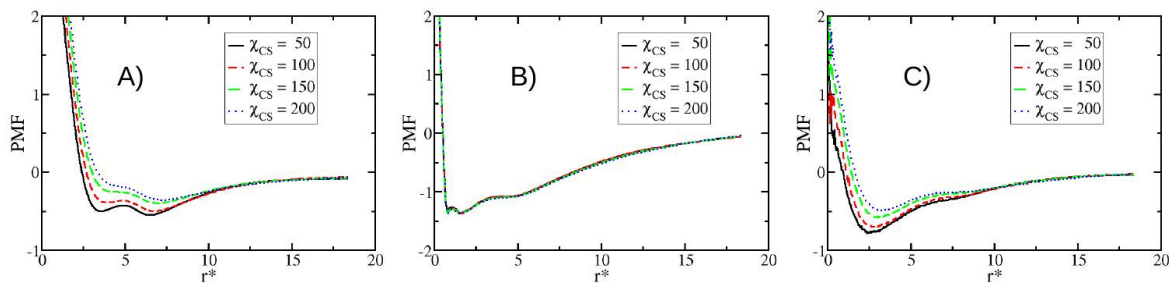


235

236 **Figure 5.** Influence of CS concentration on capsaicin on the xy plane at different concentrations of CS
 237 polymer. A) 50 chains of CS. B) 100 chains of CS. C) 150 chains of CS. D) 200 chains of CS. All quantities
 238 are reported in reduced DPD units.

239 **Potential of mean force**

240 Other properties obtained from simulations are the potentials of mean force (PMF), which are
 241 many – body interactions arising from their complex interplay beyond mean – field approximations
 242 [53]. The details about the calculation of the PMF can be found in the SI. Figure 6 shows the PMF
 243 between lecithin–CS, lecithin–capsaicin and capsaicin–CS. At higher concentrations of CS the
 244 interaction becomes weaker indicating that adsorption over the surface of the nanoliposome
 245 decreases when more CS molecules are in solution. Figure 6–B) corresponds to PMF of lecithin–
 246 capsaicin. This shows that the interaction between capsaicin and the nanoliposome is not significantly
 247 affected by the presence of CS chains, since their PMF are practically the same, making it clear that
 248 the interactions between CS and capsaicin are not the leading mechanism of nanocapsule
 249 conformation. Both Figures (Figure 6–A, 6–B) show two minimal values that are attributed to the lipid
 250 bilayer. Figure 6–C) shows the PMF between capsaicin and CS. It is evident that the attractive
 251 interactions become weaker as the quantity of CS increases. This is due to the presence of competitive
 252 adsorption which promotes the self-association between CS molecules, so that the interactions
 253 between polymer chains with the surface of nanoliposome as well as with capsaicin molecules
 254 become weaker thus causing the deposition mainly in the surface of the of the nanoliposome.



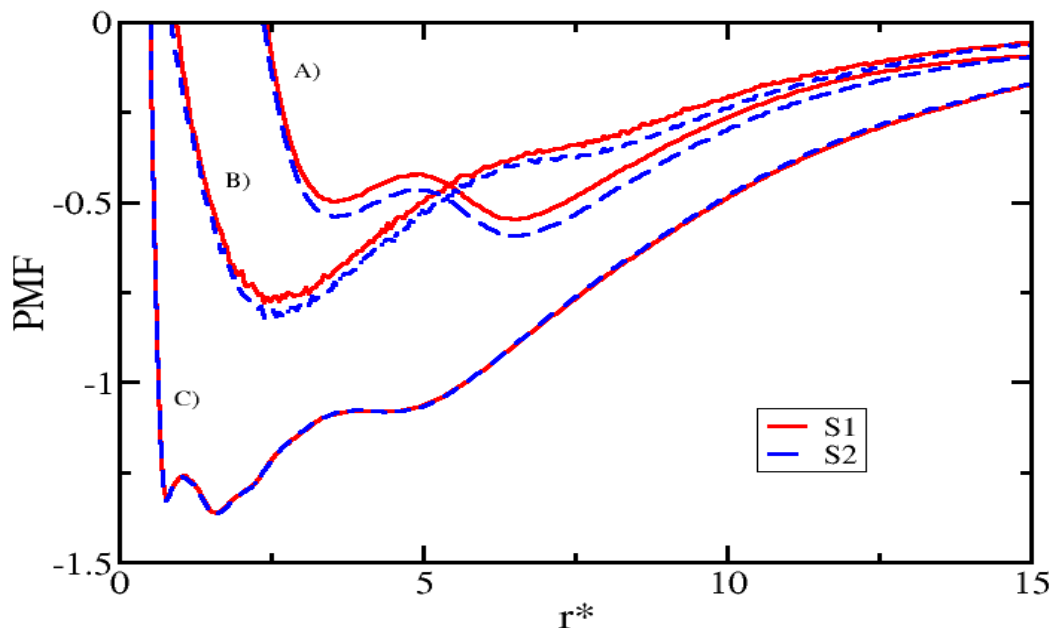
255

256 **Figure 6.** Potentials of mean force (PMF) for different concentration of CS as function of separation
 257 distance between mass centers of each molecule. A) lecithin-CS, B) lecithin-capsaicin, and C)
 258 capsaicin-CS. All quantities are expressed in reduced DPD units.

259 **Modifying the sequence of chitosan**

260 In this section we present the results obtained from the changes in the CS sequence pattern
 261 composition. The analysis presented below corresponds to a second group of simulations described
 262 at the beginning of this section. The results show that the pattern (sequence) in which the GlucNA
 263 and GlcN monomers are arranged has a clear effect on the PMF (Figure 7). We note that the PMF
 264 corresponding to CS-lecithin and CS-capsaicin indicates a favourable condition for attractiveness in
 265 the case of sequence S2 with respect to sequence S1, indicating a slight presence of cooperative effects
 266 between GlucNA units which promote the association of CS with the nanoliposome and hence with
 267 capsaicin. On the other hand, the interaction between lecithin and capsaicin is not affected or
 268 modified by these cooperative effects, so that the interaction between capsaicin and CS remains
 269 weaker than the interaction of capsaicin with lecithin.

270



271

272 **Figure 7.** PMF for the two sequences of CS used in this work, S1 (red line) and S2 (blue dotted line),
 273 to concentration of CS is 6 mM. PMF for: A) lecithin-CS, B) CS-capsaicin, and C) lecithin-capsaicin.
 274 All quantities are expressed in reduced DPD units.

275 **Mean size of nanoliposome and encapsulation efficiency (EE)**

276 Additional properties obtained from the simulations are the size of the nanoliposome and
 277 encapsulation efficiency of capsaicin. These properties are shown in Table 1. We obtained the
 278 encapsulation efficiency (EE) and mean size from the density profiles of capsaicin and lecithin,
 279 respectively, which are shown in the SI. EE is obtained from the Equation: $EE = ((CapsT -$
 280 $CapsF)/CapsT) \times 100$., where CapsT is the total concentration of capsaicin in the system and CapsF is
 281 the free capsaicin in solution.

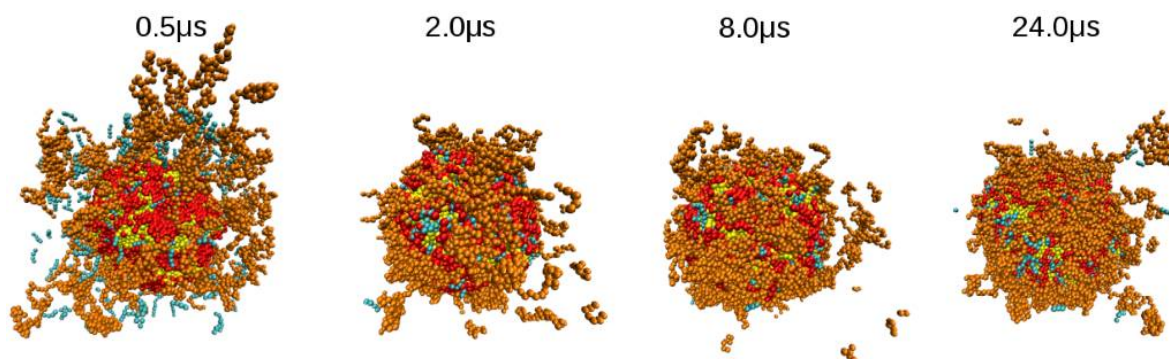
282 **Table 1.** Mean size of the nanoliposome and encapsulation efficiency (EE) as function of quantity of CS.

CS	Size (nm)	± (nm)	EE(%)	± (%)
50	17.89	0.61	96.80	0.59
100	17.95	0.46	96.27	0.69
150	18.04	0.95	96.28	0.51
200	17.90	1.00	96.71	0.61

283

284 The mean size of the simulated nanoliposome is smaller but comparable to those obtained
 285 experimentally for CS-coated oil-core nanocapsules (~ 80–250 nm) [11, 29, 50, 51]. This is an
 286 encouraging aspect of mesoscale simulation techniques, such as DPD. Additionally, the percentage
 287 of capsaicin encapsulation was very close (96%) to that reported experimentally (92%) [50].

288 Figure 8 shows snapshots obtained from the simulation trajectory where the system was
 289 monitored along time. It can be observed that capsaicin is being encapsulated inside of nanoliposome
 290 while CS is deposited on the surface. An animation of this simulation is added in the SI section where
 291 capsaicin encapsulation is clearly observed.



292

293 **Figure 8.** Snapshots of adsorption of CS on the nanoliposome at various times during simulation. In
 294 these pictures the conformation of the nanocapsule along different times can be observed. The color
 295 code in this Figure is the same as the one in Figure 2. The solvent molecules are not shown for clarity
 296 purposes. These Figures were prepared with the VMD package [47].

297 **4. Conclusions**

298 We performed DPD simulations to analyze the stability of nanocapsules formed by
 299 nanoliposomes with a polyelectrolyte shell (CS). Results obtained from density maps showed that
 300 the nanocapsule is stable with size but comparable to those of nanocapsules experimentally obtained.
 301 The information provided by the potentials of mean force showed that the interaction between
 302 capsaicin and CS is very weak compared to that with lecithin. An association between capsaicin and
 303 CS, in presence of lecithin, is not likely to occur. Under experimental conditions, the solvent may
 304 harbor other, molecular compounds that can reduce the absorption of capsaicin by the nanoliposome.

305 **Supplementary Materials:** The following are available online at www.mdpi.com/link.

306 **Acknowledgments:** This work was supported by CONACYT [Project FON.INST./44/2016]. All simulations
307 reported in this work were performed at the Supercomputer OLINKA, located at the Laboratory of Molecular
308 Bioengineering at Multiscale (LMBM), at the Universidad Autónoma del Estado de México. The authors thank
309 the financial support from CONACYT in covering the Open Access publishing costs.

310 **Author Contributions:** AGG, RLR and KATM conceived and designed the project; KATM and EMB performed
311 the simulations. JH, IHC, CV, ZD and AGG analyzed the data; JH, IHC, FMGV, WAM, RLR and AGG
312 contributed to the discussion of results. All authors contributed to the reading, writing and approval of the
313 manuscript.

314 **Conflicts of Interest:** The authors declare no conflict of interest. The founding sponsors had no role in the design
315 of the study; in the collection, analyses, or interpretation of data; in the writing of the manuscript, or in the
316 decision to publish the results.

317 References

- 318 1. Sato, A.K.; Viswanathan, M.; Kent, R.B.; Wood, C.R. Therapeutic peptides: technological advances driving
319 peptides into development. *Curr. Opin. Biotech.* **2006**, *17*, 638–642. DOI: 10.1016/j.copbio.2006.10.002.
- 320 2. Sapsford, K.E.; Algar, W.R.; Berti, L.; Gemmill, K.B.; Casey, B.J.; Oh, E.; Stewart, M.H.; Medintz, I.L.
321 Functionalizing Nanoparticles with Biological Molecules: Developing Chemistries that Facilitate
322 Nanotechnology. *Chem. Rev.* **2013**, *113*, 1904–2074. DOI: 10.1021/cr300143v.
- 323 3. Luo, Y.Y.; Xiong, X.Y.; Tian, Y.; Li, Z.L.; Gong, Y.Ch.; Li, Y.P. A review of biodegradable polymeric systems
324 for oral insulin delivery. *Drug Deliv.* **2016**, *23*, 1882–1891. <http://dx.doi.org/10.3109/10717544.2015.1052863>.
- 325 4. Hasan, M.; Messaoud, G. B.; Michaux, F.; Tamayol, A.; Kahn, C.J.F.; Belhaj, N.; Linder, M.; Arab-Tehrany,
326 E. Chitosan-coated liposomes encapsulating curcumin: Study of lipid polysaccharide interactions and
327 nanovesicles behavior. *RSC Adv.* **2016**, *6*, 45290–45304. DOI: 10.1039/C6RA05574E.
- 328 5. Janes, K.A.; Calvo, P.; Alonso, M.J. Polysaccharide colloidal particles as delivery systems for
329 macromolecules. *Adv. Drug Deliver. Rev.* **2001**, *47*, 83–97. PII: S0169-409X(00)00123-X.
- 330 6. Garcia-Fuentes, M.; Alonso, M.J. Chitosan-based drug nanocarriers: Where do we stand? *J. Control. Release*
331 **2012**, *161*, 496–504. doi: 10.1016/j.jconrel.2012.03.017.
- 332 7. Santos-Carballal, B.; Fernandez-Fernandez, E.; Goycoolea, F.M. Chitosan in non-viral gene delivery: Role
333 of structure, characterization methods and insights in cancer and rare diseases therapy. *Polymers* **2018**, *10*,
334 444. DOI: 10.3390/polym10040444
- 335 8. Guo, J.; Ping, Q.; Jiang, G.; Huang, L.; Tong, Y. Chitosan-coated liposomes: characterization and interaction
336 with leuprolide. *Int. J. Pharmaceut.* **2003**, *260*, 167–173. doi:10.1016/S0378-5173(03)00254-0.
- 337 9. Schubert, M.A.; Harms, M.; Müller-Goymann, Ch.Ch.M. Structural investigations on lipid nanoparticles
338 containing high amounts of lecithin. *Eur. J. Pharm. Sci.* **2006**, *27*, 226–236. doi:10.1016/j.ejps.2005.10.004.
- 339 10. Sonvico, F.; Cagnani, A.; Rossi, A.; Motta, S.; Di Bari, M.T.; Cavatorta, F.; Alonso, M.J.; Deriu, A.; Colombo,
340 P. Formation of self-organized nanoparticles by lecithin/chitosan ionic interaction. *Int. J. Pharmaceut.* **2006**,
341 324, 67–73. doi:10.1016/j.ijpharm.2006.06.036.
- 342 11. Mengoni, T.; Adrian, M.; Pereira, S.; Santos-Carballal, B.; Kaiser, M.; Goycoolea, F.M. A Chitosan-Based
343 Liposome Formulation Enhances the In Vitro Wound Healing Efficacy of Substance P Neuropeptide.
344 *Pharmaceutics* **2017**, *9*, 56. doi:10.3390/pharmaceutics9040056.
- 345 12. Hafner, A.; Lovrić, J.; Pepić, I.; Filipović-Grčić, J. Lecithin/chitosan nanoparticles for transdermal delivery
346 of melatonin. *J. Microencapsul.* **2011**, *28*, 807–815. DOI: 10.3109/02652048.2011.622053.
- 347 13. Tan, Q.; Liu, W.; Guo, Ch.; Zhai, G. Preparation and evaluation of quercetin-loaded lecithin-chitosan
348 nanoparticles for topical delivery. *Int. J. Nanomed.* **2011**, *6*, 1621–1630. <http://dx.doi.org/10.2147/IJN.S22411>.
- 349 14. Souza, M.P.; Vaz, A.F.M.; Correia, M.T.S.; Cerqueira, M.A.; Vicente, A.A.; Carneiro-da-Cunha, M. G.
350 Quercetin-Loaded Lecithin/Chitosan Nanoparticles for Functional Food Applications. *Food Bioprocess
351 Technol.* **2014**, *7*, 1149–1159. DOI 10.1007/s11947-013-1160-2.
- 352 15. Omwenga, E.O.; Hensel, A.; Shitandi, A.; Goycoolea, F.M.; Chitosan nanoencapsulation of flavonoids
353 enhances their quorum sensing and biofilm formation inhibitory activities against an *E.coli* Top 10
354 biosensor. *Colloid Surf B: Biointerfaces* **2018**, *164*, 125–133. doi: 10.1016/j.colsurfb.2018.01.019.

355 16. Barbieri, S.; Sonvico, F.; Como, C.; Colombo, G.; Zani, F.; Buttini, F.; Bettini, R.; Rossi, A.; Colombo, P.
356 Lecithin/chitosan controlled release nanopreparations of tamoxifen citrate: Loading, enzyme-trigger
357 release and cell uptake. *J. Control. Release.* **2013**, *167*, 276–283. <http://dx.doi.org/10.1016/j.conrel.2013.02.009>.

358 17. Mendes, A.C.; Gorzelanny, C.; Halter, N.; Schneider, S.W.; Chronakis, I.S. Hybrid electrospun chitosan-
359 phospholipids nanofibers for transdermal drug delivery. *Int. J. Pharm.* **2016**, *510*, 48–56. doi:
360 10.1016/j.ijpharm.2016.06.016

361 18. Mendes, A.C.; Shekarforoush, E.; Engwer, C.; Beerens, S.R.; Gorzelanny, C.; Goycoolea, F.M.; Chronakis I.
362 S. Co-assembly of chitosan and phospholipids into hybrid hydrogels. *Pure Appl. Chem.* **2016**, *8*, 905–916.
363 DOI:10.1515/pac-2016-0708.

364 19. Cortright, D.N.; Zallasi, A. Biochemical pharmacology of the vanilloid receptor TRPV1. An update. *Eur. J.
365 Biochem.* **2004**, *271*, 814–819. <https://doi.org/10.1111/j.1432-1033.2004.04082.x>.

366 20. Bevan, S.; Szolcsányi, J. Sensory neuron-specific actions of capsaicin: mechanisms and applications. *Trends
367 Pharmacol. Sci.* **1990**, *11*, 330–333. [https://doi.org/10.1016/0165-6147\(90\)90237-3](https://doi.org/10.1016/0165-6147(90)90237-3).

368 21. Foster, H.E.Jr.; Lake, A.G. Use of Vanilloids in Urologic Disorders. In: Abdel-Salam O. (eds) Capsaicin as a
369 Therapeutic Molecule. *Progress in Drug Research. Springer Base.* **2014**. *68*. 307–317. doi:10.1007/978-3-0348-
370 0828-6_13.

371 22. Caterina, M.J.; Schumacher, M.A.; Tominaga, M.; Rosen, T.A.; Levine, J.D.; Julius, D. The capsaicin
372 receptor: A heat-activated ion channel in the pain pathway. *Nature.* **1997**, *389*, 816–824. DOI: 10.1038/39807.

373 23. Abdel-Salam, O.M.E. (ed.). Capsaicin as a Therapeutic Molecule, *Prog. Drug Res.* **2014**. *68*. DOI: 10.1007/978-
374 3-0348-0828-6.ss

375 24. Tsukura, Y.; Mori, M.; Hirotani, Y.; Ikeda, K.; Amano, F.; Kato, R.; Ijiri, Y.; Tanaka, K. Effects of capsaicin
376 on cellular damage and monolayer permeability in human intestinal Caco-2 cells. *Biol. Pharm. Bull.* **2007**,
377 *30*, 1982–1986. <https://doi.org/10.1248/bpb.30.1982>.

378 25. Turgut, C.; Newby, B.; Cutright, T. J. Determination of Optimal Water Solubility of Capsaicin for its Usage
379 as a Non-toxic Antifoulant. *Environ. Sci. Pollut. R.* **2004**, *11*, 7–10. <https://doi.org/10.1065/espr2003.12.180>.

380 26. Choi, A.Y.; Kim, C.-T.; Park, H.Y.; Kim, H.O.; Lee, N.R.; Lee, K.E.; Gwak, H.S. Pharmacokinetic
381 characteristics of capsaicin-loaded nanoemulsions fabricated with alginate and chitosan. *J. Agric. Food
382 Chem.* **2013**, *61*, 2096–2102. DOI: 10.1021/jf3052708.

383 27. Kaiser, M.; Kirsch, B.; Hauser, H.; Schneider, D.; Seuß-Baum, I.; Goycoolea, F.M. In Vitro and Sensory
384 Evaluation of Capsaicin-Loaded Nanoformulations. *PLoS ONE*, **2015**, *10*, e0141017.
385 doi:10.1371/journal.pone.0141017.

386 28. Choi, A.; Kim, C.; Cho, Y.; Hwang, J.; Kim, C. Characterization of Capsaicin-Loaded Nanoemulsions
387 Stabilized with Alginate and Chitosan by Self-assembly. *Food and Bioprocess Technology* **2011**, *4*, 1119–1126.
388 <https://doi.org/10.1007/s11947-011-0568-9>.

389 29. Goycoolea, F.M.; Valle-Gallego, A.; Stefani, R.; Menchicchi, B.; David, L.; Rochas, C.; Santander-Ortega,
390 M.J.; Alonso, M.J. Chitosan-based nanocapsules: physical characterization, stability in biological media and
391 capsaicin encapsulation. *Colloid Polym. Sci.* **2012**, *290*, 1423–1434. DOI 10.1007/s00396-012-2669-z.

392 30. Santander-Ortega, M.J.; Peula-García, J.M.; Goycoolea, F.M.; Ortega-Vinuesa, J.L. Chitosan nanocapsules:
393 Effect of chitosan molecular weight and acetylation degree on electrokinetic behaviour and colloidal
394 stability. *Colloid Surface B* **2011**, *82*, 571–580. doi:10.1016/j.colsurfb.2010.10.019.

395 31. Fu, X.; Liu, H.; Liu, Y.; Liu, Y. Application of Chitosan and Its Derivatives in Analytical Chemistry: A Mini-
396 Review. *Journal of Carbohydrate Chemistry*, **2013**, *32*, 463–474, DOI: 10.1080/07328303.2013.863318.

397 32. Hu, L.; Sun, Y.; Wu, Y. Advances in chitosan-based drug delivery vehicles. *Nanoscale*, **2013**, *5*, 3103–3111.
398 DOI: 10.1039/c3nr00338h.

399 33. Prego, C.; Fabre, M.; Torres, D.; Alonso, M.J. Efficacy and mechanism of action of chitosan nanocapsules
400 for oral peptide delivery. *Pharm. Res.* **2006**, *23*, 549–556. DOI: 10.1007/s11095-006-9570-8.

401 34. Gonzalez-Paredes, A.; Torres, D.; Alonso, M.J. Polyarginine nanocapsules: A versatile nanocarrier with
402 potential in transmucosal drug delivery. *Int. J. Pharmaceut.* **2017**, *529*, 474–485.
403 <https://doi.org/10.1016/j.ijpharm.2017.07.001>.

404 35. López-Montilla, J.C.; Herrera-Morales, P.E.; Pandey, S.; Shah, D.O. Spontaneous emulsification:
405 Mechanisms, physicochemical aspects, modeling, and applications. *J. Dispersion Sci. Technol.* **2002**, *23*, 219–
406 268. <https://doi.org/10.1080/0193269020894202>.

407 36. Vicente, S.; Peleteiro, M.; Díaz-Freitas, B.; Sanchez, A.; González-Fernández, Á.; Alonso, M.J. Co-delivery
408 of viral proteins and a TLR7 agonist from polysaccharide nanocapsules: A needle-free vaccination strategy.
409 *J. Controlled Release* **2013**, *172*, 773–781. doi: 10.1016/j.jconrel.2013.09.012.

410 37. Vicente, S.; Diaz-Freitas, B.; Peleteiro, M.; Sanchez, A.; Pascual, D. W.; Gonzalez-Fernandez, A.; Alonso,
411 M.J. A Polymer/Oil Based Nanovaccine as a Single-Dose Immunization Approach. *PLoS ONE* **2013**, *8*, 1–8.
412 doi:10.1371/journal.pone.0062500.

413 38. Al-Remawi, M.; Elsayed, A.; Maghrabi, I.; Hamaidi, M.; Jaber, N. Chitosan/lecithin liposomal nanovesicles
414 as an oral insulin delivery system, *Pharmaceutical Dev. Technol.* **2016**, *3*, 390–398.
415 <http://dx.doi.org/10.1080/10837450.2016.1213745>.

416 39. Ilk, S.; Saglam, N.; Özgen, M. Kaempferol loaded lecithin/chitosan nanoparticles: preparation,
417 characterization, and their potential applications as a sustainable antifungal agent. *Artif. Cells. Nanomed.*
418 and *Biotechnol.* **2016**, *45*, 907–916. <http://dx.doi.org/10.1080/21691401.2016.1192040>.

419 40. Laye, C.; McClements, D.J.; Weiss, J. Formation of Biopolymer-Coated Liposomes by Electrostatic
420 Deposition of Chitosan. *J. Food Sci.* **2008**, *73*, N7–N15. doi: 10.1111/j.1750-3841.2008.00747.x.

421 41. Gama Goicochea, A.; Briseño M. Application of Molecular Dynamics Computer Simulations to Evaluate
422 Polymer – Solvent Interactions. *J. Coat. Technol. Res.* **2023**, *9*, 279. DOI: 10.1007/s11998-011-9364-8.

423 42. Gama Goicochea, A.; Alas Guardado, S. J. Computer simulations of the mechanical response of brushes on
424 the surface of cancerous epithelial cells. *Sci. Rep.* **2015**, *5*, 13218. DOI: 10.1038/srep13218.

425 43. Gama Goicochea, A.; Alarcón, F. Solvation force induced by short range, exact dissipative particle
426 dynamics effective surfaces on a simple fluid and on polymer brushes. *J. Chem. Phys.* **2011**, *134*, 014703.
427 DOI: 10.1063/1.3517869.

428 44. Pastorino, C.; Gama Goicochea, A. Dissipative Particle Dynamics: A Method to Simulate Soft Matter
429 Systems in Equilibrium and Under Flow. *Selected Topics of Computational and Experimental Fluid Mechanics,*
430 *Environmental Science and Engineering*, Springer International Publishing Switzerland **2015**, 51–79. DOI
431 10.1007/978-3-319-11487-3_3.

432 45. Soddeemann, T.; Dunweg, B.; Kremer, K. Dissipative particle dynamics: A useful thermostat for equilibrium
433 and nonequilibrium molecular dynamics simulations. *Phys. Rev. E. Stat Nonlin Soft Matter Phys.* **2003**, *68*,
434 046702. DOI: 10.1103/PhysRevE.68.046702.

435 46. Terrón-Mejía, K.A.; López-Rendón, R.; Goicochea, A.G. SIMES: SImulation at MESoscopic Scale—
436 Accelerating Dissipative Particle Dynamics Simulations on Graphical Processing Units. *The 3rd International*
437 *Electronic and Flipped Conference on Entropy and Its Applications (ECEA 2016)*, Sciforum Electronic Conference
438 Series, **2016**, *3*, DOI: 10.3390/ecea-3-A001.

439 47. Humphrey, A.; Dalke, A.; Schulten, K. VMD – Visual Molecular Dynamics. *J. Mol. Graphics* **1996**, *14*, 33–38.
440 [https://doi.org/10.1016/0263-7855\(96\)00018-5](https://doi.org/10.1016/0263-7855(96)00018-5).

441 48. Hsu, A.; Whu, S.W.; Tsai, C.-L.; Wu, Y.-H.; Chen, H.-W.; Hsieh, K.-H. Chitosan as Scaffold Materials: Effects
442 of Molecular Weight and Degree of Deacetylation. *Journal of Polymer Research* **2004**, *11*, 141–147.
443 <https://doi.org/10.1023/B:JPOL.0000031080.70010.0b>.

444 49. Kweon, J.; Park, M.; Chung, J.; Na, H.; Choi, Park, Y.II. Effects of the Molecular Weight and the Degree of
445 Deacetylation of Chitosan Oligosaccharides on Antitumor Activity. *Int. J. Mol. Sci.* **2011**, *12*, 266–277;
446 doi:10.3390/ijms12010266.

447 50. Kaiser, M.; Pereira, S.; Pohl, L.; Ketelhut, S.; Kemper, B.; Gorzelanny, C.; Galla, H.-J.; Moerschbacher, B.M.;
448 Goycoolea, F.M. Chitosan encapsulation modulates the effect of capsaicin on the tight junctions of MDCK
449 cells. *Sci. Rep.* **2014**, *5*, 10048. DOI: 10.1038/srep10048.

450 51. Shin, G.H.; Chung, S.K.; Kim, J.T.; Joung, H.J.; Park, H.J. Preparation of chitosan-coated nanoliposomes for
451 improving the mucoadhesive property of curcumin using the ethanol injection method. *J. Agric. Food Chem.*
452 **2013**, *61*, 11119–11126. DOI: 10.1021/jf4035404.

453 52. Goycoolea, F.M.; Milkova, V. Electrokinetic behavoir of chitosan adsorbed on o/w nanoemulsion droplets.
454 *Colloids and Surfaces A: Physicochem Eng. Aspects.* **2017**, *519*, 205–211. doi:10.1016/j.colsurfa.2016.05.093.

455 53. Catarino Centeno, R.; Pérez, E.; Gama Goicochea, A. On the potential of mean force of a sterically stabilized
456 dispersion. *J. Coat. Technol. Res.* **2014**, *11*, 1023. DOI: 10.1007/s11998-014-9600-0.